Fast tissue investigation using label-free point- and angle-scanning widefield multiphoton microscopies

Mikko J. Huttunen[1] **and Antti Kiviniemi**[1]

[1]*Photonics Laboratory, Physics Unit, Tampere University, Tampere, Finland*

Tel: (35850) 4921272, e-mail: mikko.huttunen@tuni.fi

ABSTRACT

Multiphoton microscopy has recently emerged as a powerful high-resolution and label-free imaging modality to study biological specimens *in-vivo*. Multiphoton modalities require minimal sample preparation showing potential in applications benefitting from fast imaging protocols, such as in medical diagnosis. Here, we overview our recent work on this topic focusing on technique development that could provide fast imaging capabilities to rival conventional imaging modalities. In particular, we demonstrate a novel widefield multiphoton technique that greatly facilitates wavelength-scanning multimodal imaging.

Keywords: nonlinear imaging, multiphoton, two-photon excitation fluorescence, second-harmonic generation.

1. INTRODUCTION

Multiphoton microscopy (MPM) techniques have recently emerged as powerful imaging modalities to investigate biological specimens [1, 2]. The main advantages of MPM are the intrinsic optical sectioning, and the possibility to image and investigate live biological samples label-free and with good contrast [3]. Subsequently, MPM requires minimal sample preparation, and for some specimens (such as human skin) can even be performed *in-vivo* [4, 5]. It is therefore not surprising that MPM has recently gained popularity particularly in the field of medical diagnosis [4, 5].

The two by far most commonly utilized MPM modalities are second-harmonic generation (SHG) and two-photon excitation fluorescence (TPEF) microscopies [3]. During the process of SHG two incident photons oscillating at fundamental frequency ω are combined into a single photon oscillating at doubled frequency 2ω. This process does not require presence of real molecular energy states but occurs via virtual energy levels [6]. Consequently, the excitation does not alter the state of the investigated system making SHG a coherent process. SHG microscopy is commonly used to investigate organization of collagen and elastin proteins, which are major components of the extracellular matrix (ECM) [7–10]. TPEF, on the other hand, occurs via real molecular energy states of the system and is therefore an incoherent process. Because many endogenous fluorophores (such as flavins, melanins, retinal, elastin and keratin) are present in biological tissues [11], TPEF microscopy allows to visualize organization of tissues, and facilitates the non-invasive and label-free imaging of cellular morphology and organization. These two MPM modalities can be performed simultaneously with ease allowing high contrast, label-free and minimally invasive imaging of tissues. For example, combined SHG and TPEF microscopy have been utilized to investigate remodeling of the ECM during cancer progression [12]. The compatibility of MPM for in-vivo tissue investigations has also been demonstrated [4, 13].

When performing MPM, signals of nonlinear origin collected via different imaging modalities, such as TPEF and SHG, typically overlap spectrally. Separation of the spectrally narrow SHG signals from spectrally broad TPEF signals is normally achieved using spectral filters. While this approach works well for MPM using a single incident wavelength, it is not trivial to transfer this approach, for example, to perform wavelength-scanning MPM. However, because wavelength-scanning MPM would provide improved contrast by for example allowing visualization of several different endogeneous fluorophores, it would be beneficial to develop such easy-to-use and fast MPM techniques.

Here, we introduce a novel wide-field MPM technique that can potentially address the issues related to wavelength-scanning MPM. We call the technique angle-scanning widefield multiphoton microscopy (ASWMPM), that allows to separate the TPEF and SHG signals from each other without the need of any spectral filters. ASWMPM takes advantage of the principle that fluorescent light (here from TPEF) is spatially incoherent whereas light due to process of SHG is spatially coherent. We show a proof-of-principle demonstration from mammalian bone specimens and discuss the potential of the technique for fast MPM tissue visualization and subsequent characterization.

2. ANGLE-SCANNING WIDEFIELD MULTIPHOTON MICROSCOPY

Use of ASWMPM requires to use a spatially coherent light source that is associated with very high peak intensities, i.e. a pulsed laser. Because ASWMPM is a widefield technique, the sample is illuminated by using a collimated input beam, and the scattered light is imaged using a camera. Because we are only interested of the signals arising from the multiphoton processes occurring in the sample, the incident pump beam is prevented from reaching the

imaging camera by using a spectral filter. Depending on the sample characteristics, both SHG and TPEF nonlinear optical processes often take place resulting in an MPM image that is an overlap of TPEF and SHG images. Usually, these two images are separated from each other by placing into the microscope's imaging arm additional dichroic mirrors and/or spectral filters. However, it is also possible to separate these two signals by taking advantage of the momentum conservation of the coherent SHG process. In terms of imaging, this means that the spatial frequencies k that participate to the image formation depend on the illumination angle θ, which fact is often utilized for example in ptychography or in optical tomography [14, 15].

The sample is first illuminated at normal incidence ($\theta = 0°$) and an image is captured [see Fig. 1a)]. Next the illumination angle θ is changed and another image is taken [see Fig. 1b)]. This process is repeated several times while varying the illumination angle θ [see Fig. 1c)]. All acquired individual MPM images contain both SHG and TPEF signals. However, the TPEF signals (see red solid lines) remain unchanged whereas the SHG signals (see green dotted lines) depend on θ. This occurs because TPEF is an incoherent process, and consequently it does not give rise to a speckle pattern. Only the SHG signals in each MPM image have a speckle pattern contribution to the image. By then taking a sum of all the MPM images, a speckle-free MPM image is formed containing both SHG and TPEF contributions. Each individual MPM image differs from this sum of MPM images only by the SHG speckle pattern. Now, by taking the absolute difference of each MPM image with the sum of MPM images, the SHG speckle is separated from the TPEF part. Finally, by summing these speckled SHG images, a speckle-free SHG image is obtained.

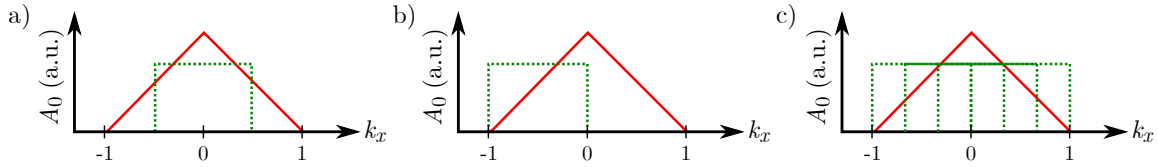

Figure 1. One-dimensional representations of the collected spatial frequencies for TPEF (red solid lines) and SHG (dotted green lines). The transfer function of the TPEF imaging modality is triangular and independent of the illumination angle θ of the excitatiom beam. a)–c) The transfer function of the SHG modality however depends on θ. This difference between the modalities allows to separate the information contained in the overall image, which is the sum of these contributions. c) By collecting information as a function of θ, the TPEF and SHG images of similar resolution can be extracted.

In order to demonstrate the above-introduced ASWMPM technique, we performed widefield MPM with a custom-built microscope using a pulsed titanium-sapphire laser oscillator (Chameleon Vision, $\lambda = 850$ nm, pulse length 200 fs, repetition rate 80 MHz and mean power 3 W) as our source laser. A dual-mirror galvanometer scanner was used to steer the laser beam through a scan lens (Thorlabs, LSM05-BB) which focused the laser beam onto the back focal plane of the microscope objective. This produced a collimated laser beam incident on the sample. In order to minimize excessive sample heating, the mean power of the beam at the sample was kept at around 1 W or less. The azimuthal and polar angles of this beam were computer-controlled with the high-speed galvanometer scanner. Our microscope operated in epi-illumination configuration and the back-propagated light was reflected using a dichroic beamsplitter into a tube lens and bandpass filters before finally entering our CMOS camera (see Fig. 2). The dichroic beamsplitter and bandpass filters blocked the fundamental laser beam from entering the camera and passed SHG and most of TPEF light that oscillated with higher frequencies than the fundamental laser beam.

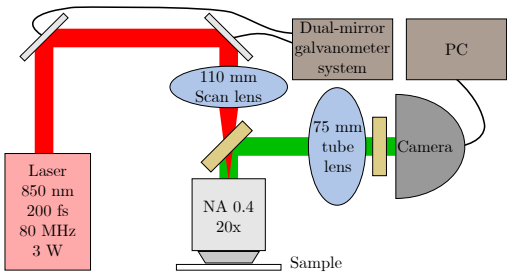

Figure 2. Incident beam was guided using a dual-mirror scanner into a scan lens focusing the beam into the back focal plane of the objective lens. Backward emitted MPM signals were guided into the camera by using a dichroic mirror and a tube lens ($f = 75$ mm). Bandpass filters were used to block the fundamental laser beam from entering the camera. MPM images were recorded as a function of illumination angle θ allowing separation of the SHG and TPEF images from each other.

In our experiment, we used a plan achromat NA = 0.4 20× objective (Olympus) and a f = 75 mm achromatic doublet (Thorlabs, AC508-075-A-ML) as the tube lens resulting in a 8.33× total magnification of our imaging system. Our camera (The Imaging Source, DMK 33UX264) had a pixel size of 3.45 µm which made a single image pixel width to correspond to 414 nm. For normally-incident coherent illumination, diffraction limit (λ/NA) for SHG wavelength of 425 nm is 1063 nm, while the resolution for angle-scanning SHG and incoherent TPEF modalities was calculated to be roughly half of that (532 nm). In total, we recorded 34 images using different illumination directions using an exposure time of 2 seconds and a camera gain of 9 dB. The illumination direction was controlled using a high-speed dual-mirror scanner resulting in total image capture time of 70 seconds. A slice from a mammalian bone cortex was used as a test sample (see Fig. 3), because fibrous collagen proteins, a major constituent of cortical bone, are known to be efficient SHG emitters. Interestingly, we see that the recorded MPM signals depend on the illumination angle allowing to separate these contributions (SHG signal) from the unchanged signal contribution (TPEF signal). We note that a relatively strong MPM background is visible in the recorded images. We attribute this signal to be mostly out-of-focus blur arising from the widefield excitation, that could potentially be reduced by deconvolution techniques [16].

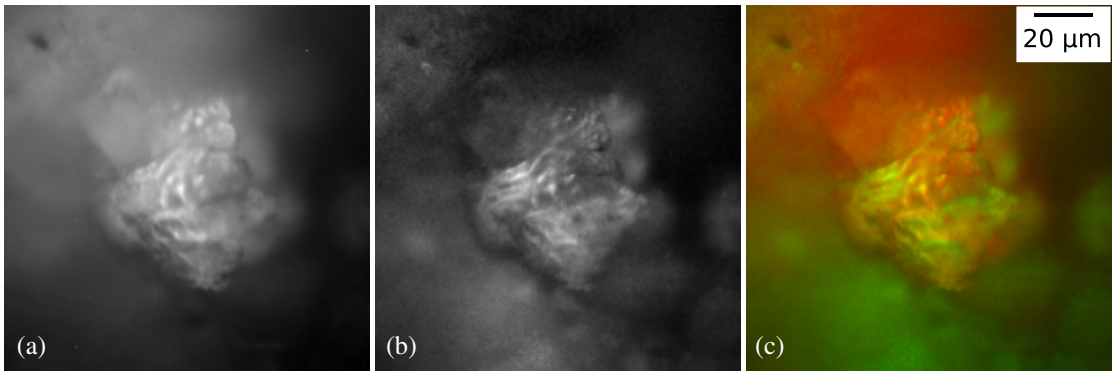

Figure 3. MPM images of a mammal bone cortex. (a) Sum of MPM images recorded using 34 different illumination directions includes both SHG and TPEF contributions. (b) SHG image separated from image (a). (c) Combined TPEF (red) and SHG (green) image. Intensity scales are different between images and color channels.

3. LABEL-FREE MULTIPHOTON MICROSCOPY FOR FAST TISSUE VISUALIZATION

In addition to the above proof-of-principle demonstration of ASWMPM, where the illumination of the sample is performed using a collimated beam, we have also performed more conventional point-scanning MPM using camera-based detection. Using point-scanning excitation, considerably weaker excitation powers can be used (∼10 mW) than using ASWMPM (∼1 W). In addition, the intrinsic optical sectioning capabilities of point-scanning MPM reduce the out-of-focs blur present in ASWMPM. A potential disadvantage of point-scanning modalities is the fact that the imaging speeds are dictated by the speed of the scanners. We estimate that using our system, faster imaging could potentially be achieved via ASWMPM. However, we note that by performing point-scanning MPM using multiple focal points, very fast volumetric *in-vivo* MPM imaging has been recently demonstrated [17]. Some advanced MPM modalities also require specific polarization states to be used during imaging [18, 19]. We note that it might be easier to implement such techniques using widefield MPM, where a collimated beam is used to excite the sample. We think this to be the case especially when wavelength-scanning polarization sensitive microscopy is performed [20].

We are specifically interested in applying fast and label-free MPM to speed-up visualization of large, millimeter scale, histopathological sample slides, that often provide first cues of disease in medical diagnosis. Recent advances in machine learning are revolutionizing the field of histopathology by automating many image processing tasks earlier performed manually by histopathologists [10]. We believe that by combining a label-free imaging modality requiring minimal sample preparation, or providing even *in-vivo* capabilities [4], with automated and fast deep-learning-based image analysis, current cost effectiveness of histopathology could be dramatically improved. Here, the demonstrated ASWMPM seems promising, especially when combined with amplified laser systems enabling imaging using milliwatt-level imaging powers thus potentially enabling *in-vivo* studies [21].

4. CONCLUSION

We have demonstrated a widefield multiphoton microscopy technique that allows to separate coherent second-harmonic generation signals from incoherent endogeneous two-photon excitation fluorescence signals without the need to use spectral filtering. This advantage facilitates wavelength-scanning multiphoton microscopy, that

could potentially improve the achievable contrast of such modalities and facilitate development of novel multiphoton imaging modalities. We have also compared the advantages and disadvantages of point-scanning and angle-scanning widefield multiphoton microscopy modalities for fast and label-free imaging of biological tissues. In particular, we have discussed the potential to apply multiphoton microscopy to large-scale imaging in order to speed-up visualization of whole histopathology slides.

ACKNOWLEDGEMENTS

We acknowledge the support of the Academy of Finland (Grant No. 308596) and the Flagship of Photonics Research and Innovation (PREIN) funded by the Academy of Finland (Grant No. 320165). AK acknowledges also the support of Vilho, Yrjö and Kalle Väisälä Foundation of the Finnish Academy of Science and Letters.

References

1. W. R. Zipfel, R. M. Williams, and W. W. Webb, "Nonlinear magic: Multiphoton microscopy in the biosciences," *Nat. Biotechnol.* vol. 21, pp. 1369–1377, 2003.
2. D. Débarre et al., "Imaging lipid bodies in cells and tissues using third-harmonic generation microscopy," *Nat. Methods*, vol. 3, pp. 47–53, 2006.
3. E. E. Hoover and J. A. Squier, "Advances in multiphoton microscopy technology," *Nat. Photonics*, vol. 7, pp. 93–101, 2013.
4. K. Koenig and I. Riemann, "High-resolution multiphoton tomography of human skin with subcellular spatial resolution and picosecond time resolution," *J. Biomed. Opt.* vol. 8, p. 432, 2003.
5. S. W. Perry, R. M. Burke, and E. B. Brown, "Two-photon and second harmonic microscopy in clinical and translational cancer research," *Ann. Biomed. Eng.* vol. 40, pp. 277–291, 2012.
6. R. W. Boyd. *Nonlinear optics*. San Diego: Academic Press, 2003.
7. P. P. Provenzano et al., "Collagen reorganization at the tumor-stromal interface facilitates local invasion," *BMC Med.* vol. 4, pp. 1–15, 2006.
8. X. Chen et al., "Second harmonic generation microscopy for quantitative analysis of collagen fibrillar structure," *Nat. Protoc.* vol. 7, pp. 654–669, 2012.
9. M. J. Huttunen et al., "Automated classification of multiphoton microscopy images of ovarian tissue using deep learning," *J. Biomed. Opt.* vol. 23, p. 066002, 2018.
10. M. J. Huttunen et al., "Multiphoton microscopy of the dermoepidermal junction and automated identification of dysplastic tissues with deep learning," *Biomed. Opt. Express*, vol. 11, pp. 186–199, 2020.
11. W. R. Zipfel et al., "Live tissue intrinsic emission microscopy using multiphoton-excited native fluorescence and second harmonic generation," *Proc. Natl. Acad. Sci.* vol. 100, pp. 7075–7080, 2003.
12. N. D. Kirkpatrick, M. A. Brewer, and U. Utzinger, "Endogenous optical biomarkers of ovarian cancer evaluated with multiphoton microscopy," *Cancer Epidemiol. Biomarkers Prev.* vol. 16, pp. 2048–2057, 2007.
13. R. B. Saager et al., " In vivo measurements of cutaneous melanin across spatial scales: using multiphoton microscopy and spatial frequency domain spectroscopy," *J. Biomed. Opt.* vol. 20, p. 066005, 2015.
14. G. Zheng, R. Horstmeyer, and C. Yang, "Wide-field, high-resolution Fourier ptychographic microscopy," *Nat. Photonics*, vol. 7, pp. 739–745, 2013.
15. B. Simon et al., "Tomographic diffractive microscopy with isotropic resolution," *Optica*, vol. 4, pp. 460–463, 2017.
16. J. G. McNally et al., "Three-dimensional imaging by deconvolution microscopy," *Methods A Companion to Methods Enzymol.* vol. 19, pp. 373–385, 1999.
17. K.-J. Hsu et al., "Millisecond two-photon optical ribbon imaging for small-animal functional connectome study," *Opt. Lett.* vol. 44, pp. 3190–3193, 2019.
18. S. Brasselet, "Polarization-resolved nonlinear microscopy: application to structural molecular and biological imaging," *Adv. Opt. Photonics*, vol. 3, pp. 205–271, 2011.
19. H. Lee et al., "Chiral imaging of collagen by second-harmonic generation circular dichroism," *Biomed. Opt. Express*, vol. 4, pp. 909–916, 2013.
20. M. Y. Chen et al., "Resonant nonlinear microscopy reveals changes in molecular level chirality in native biological tissues," *Opt. Commun.* vol. 422, pp. 56–63, 2018.
21. C. Macias-Romero et al., "Wide-field medium-repetition-rate multiphoton microscopy reduces photodamage of living cells," *Biomed. Opt. Express*, vol. 7, pp. 1458–1467, 2016.